RESEARCH REPORTS

PHOTOELASTIC ANALYSIS OF THE MAXIMUM STRESS IN A WIDE PLATE WITH AN ASYMMETRICALLY REINFORCED CIRCULAR HOLE UNDER TENSION-EFFECTS OF ROUNDED CORNER AT HOLE EDGE

MASAICHIRŌ SEIKA and KIYOSHI ISOGIMI

Department of Mechanical Engineering

(Received October 13, 1970)

Introduction

The stress concentrations around circular holes in plates are frequently reduced by means of reinforcing rings placed symmetrically or asymmetrically with respect to the plates. In the previous papers[1)~4)], the stresses at the edges of holes reinforced asymmetrically with stiffening rings under uniaxial tension field were analysed by the photoelastic stress freezing method. In those studies, however, a stiffening ring was placed only on one side of a wide plate and no rounded corner was given at the hole edge on the flat side of the plate. As is observed in various pressure vessels, the rounded corner is given frequently at the hole edge on the flat side. Sufficient information on the effect of radius of curvature of the rounded corner on the maximum stress has not been presented.

In this paper, the photoelastic stress-freezing and slicing technique was applied to obtain the maximum stress at the edge of a reinforced circular hole in a wide plate under tension. The reinforcing ring was placed on one side of the plate and the hole periphery on the flat side of the plate was provided with rounded corners of various radii. Test models used were made from an epoxy resin and were fabricated by casting so as to make the ring and plate one body, using a mould of curing silicone-rubber. The experiment was performed on the rings of various dimensions, and the radius of curvature at the rounded corner effective in reducing the maximum stress was studied in connection with the optimum reinforcement. The results herein obtained are available for design data of reinforced openings in pressure vessels, diameters of which are much larger than those of the openings.

Experimental Procedure

Test models taken out from moulds were annealed to remove initial stresses and then were finished by machining in the form shown in Fig. 1. Nominal dimensions of the models tested are shown in Table 1. If the width of a plate having a central circular hole is not less than four diameters of the hole, the

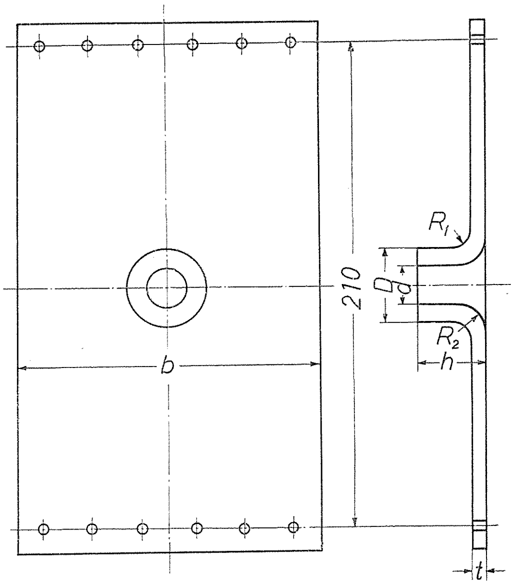

FIG. 1. Form of test model.

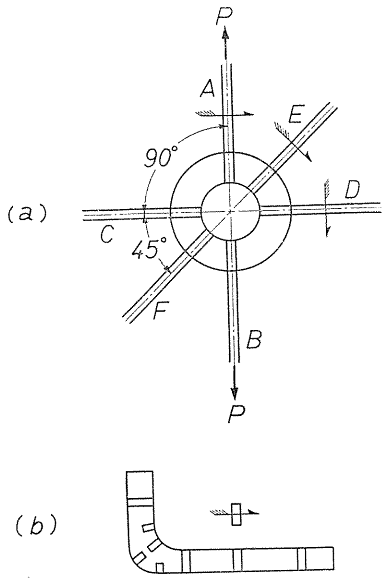

FIG. 2. Methods of slicing: (a) Slice I, (b) Slice II.

TABLE 1. Nominal Dimensions of Test Models

b mm	t mm	D mm	d mm	h mm	R_1 mm	R_2 mm	d/D	h/t	R_1/t	R_2/t
				6	0			1	0	
			9			2	0.3			0.33
				12	2			2	0.33	
120	6	30	15			5	0.5			0.83
				18	5			3	0.83	
			21			10	0.7			1.67
				24	10			4	1.67	

edges of the plate have little effect on the maximum stress occurring at the hole edge[5]. Since the width of the plates, b, examined is four times as large as the outer diameter of the ring, D, the results herein obtained may be approximated to those of an infinite plate.

All of the models were loaded in a temperature controlled oven by means of a dead weight. To avoid a certain amount of restraint to the bending tendency about the loading edges, which is brought by presence of asymmetrical reinforcements, knife-edge pivots were used at both the top and bottom connections.

The stress-freezing procedure was carried out by heating to the critical temperature (135°C), holding for about 2 hr and cooling to room temperature at a rate of 5°C/hr.

In order to obtain the stress distributions on the surfaces of the plates and rings, two kinds of slice were taken from the stress-frozen models. The location of Slice I about 3 mm-thick relative to the model is shown in Fig. 2 (a). The middle surfaces of these slices contained the geometric axis of the ring. Slice II about 2 mm-thick was taken in a direction perpendicular to the plane of Slice I and contained each location to be measured in the middle as shown in Fig. 2 (b). The measurement of fringe orders in slices was performed in a immersion bath. Integral values of the fringe orders were measured by shaving the edges of slices in wedges and fractional values were obtained by use of the Tardy method.

In this experiment, the stresses σ_n, σ_t on the inside and outside surfaces of the models were measured by use of the two kinds of slices mentioned in the foregoing, where σ_n was the stress normal to the plane of Slice I and σ_t was in the plane of the slice and tangent to the boundary. The results of the tests were expressed by those stresses divided by the nominal stress σ_0 $(=P/bt)$.

Experimental Results and Conclusion

As an example, dark field frozen-stress patterns in Slice I are shown in Fig. 3.

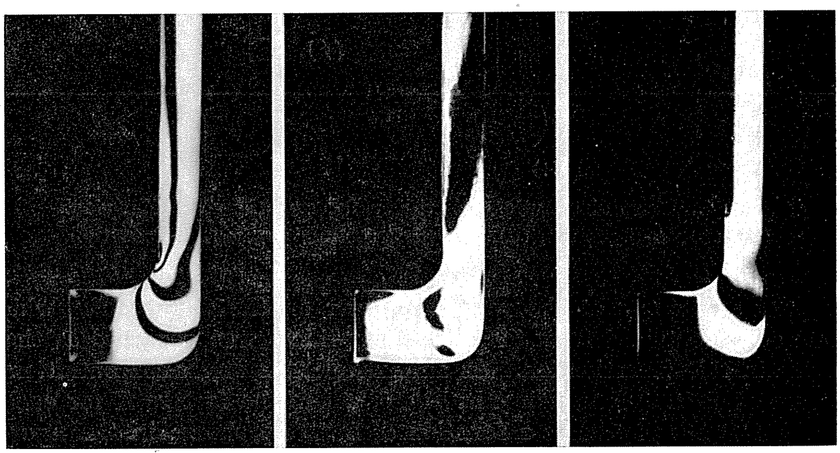

(a) A-B section (b) C-D section (c) E-F section

$h/t=3$, $d/D=0.3$, $R_1/t=R_2/t=0.83$, $P=10$ kg

FIG. 3. Dark-field frozen-stress patterns for Slice I.

The stress distributions on the hole edge and near the reinforcement were obtained by varying the radius of curvature of the rounded corner at the hole edge. As an example, Fig. 4 shows the stress distributions on the surfaces of the plate and ring for the case of $h/t=3$, $d/D=0.3$ and $R_1/t=R_2/t=0.83$. As shown in the figures, the maximum stress is the normal stress σ_n occurring at the rounded corner on the C-D section. The tangential stress σ_t in the vicinity of fillet-end of the plate on the A-B section is the next to the maximum stress in magnitude. At the hole edge on the A-B section, the maximum compressive stress σ_n occurs. The stresses on the E-F section hold almost middle in magnitude, comparing to those on the other two sections. It is found that the locations, where the stress distribution on each section is not disturbed in the plate, are distant about one and a half times the outer diameter of the ring from the axis of the hole. Within the range of the present experiment, the tendency of the stress distributions for the other models tested was quite similar to that described by the example.

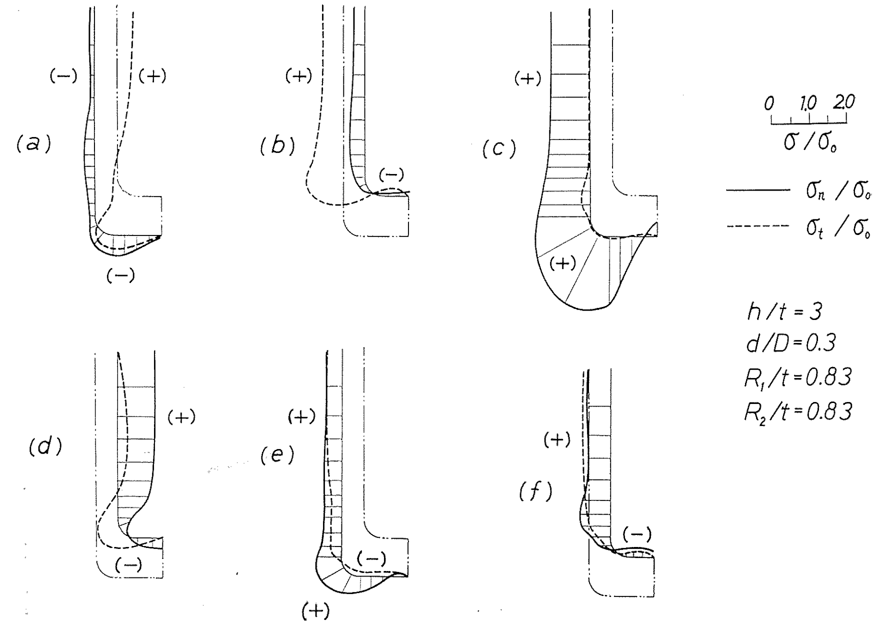

FIG. 4. Stress distributions on the surfaces of the plate and ring. (a), (b); A-B section, (c), (d); C-D section, (e), (f); E-F section.

The peak stress (σ_n) at the rounded corner on the C-D section, which was the actual stress obtained from the slice 2 mm-thick, was regarded as the maximum stress in this investigation. As an example, the stress-concentration factor for the case of $R_1/t=0.83$ is shown in Fig. 5, where the factors K for each value of R_2/t and d/D are plotted as a function of h/t. As shown in the figures, the factors K are reduced with increase of h/t and become almost constant for $h/t>3$. This indicates that if the height of a reinforcing ring is taken to be three times as large as the plate thickness, the stress concentration at the hole edge can be relieved effectively. This tendency was quite similar for the other values of R_1/t examined.

Figure 6 shows the relation between the stress-concentration factor and the radius of curvature of the rounded corner for the case of $h/t=3$, where the factors K for each value of R_1/t and d/D are plotted as a function of R_2/t. In these figures, values of K for $R_2/t=0$ were obtained in the previous paper[4]. As is shown in the figures, the factors K are reduced with increase of R_2/t and become almost constant for $R_2/t>1$. Namely, though the radius of curvature more than the plate thickness is provided at the corner of the hole periphery, the effective reduction of the stress concentration cannot be expected.

As an example, Fig. 7 shows the relation between the compressive normal stress (σ_n) on the A-B section and h/t for the case of $R_1/t=0.83$, where the ordinate K' represents the ratio of the compressive stress σ_n to the nominal stress σ_0. In these figures, values of the compressive stresses were measured at the locations corresponding to those on the C-D section at which the maximum stresses yield. Combining properly the results in Fig. 5 and those in Fig. 7 for each value

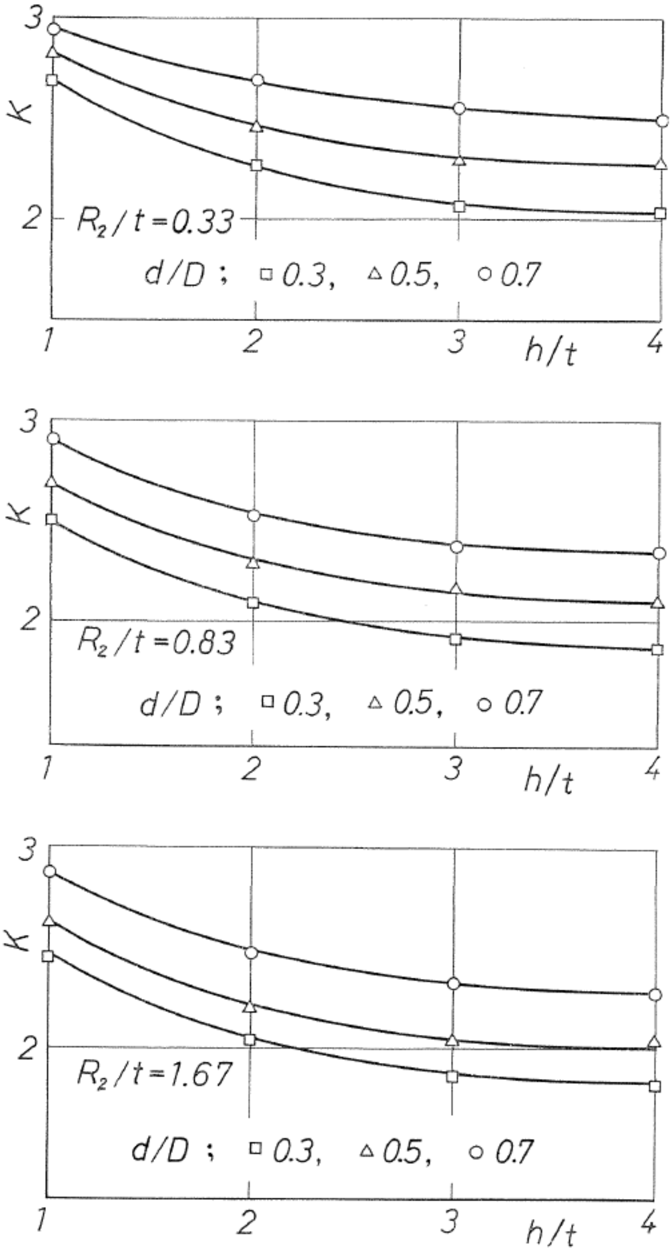

FIG. 5. Stress-concentration factor K for $R_1/t=0.83$.

of R_2/t and h/t, the stress concentration at the periphery of the reinforced hole in a wide plate can be obtained under various loading conditions. For example, the stress-concentration factors for biaxial tension of the ratio $1:1/2$ and pure shear for the case of $R_1/t=R_2/t=0.83$ are shown in Fig. 8, where $K+1/2\,K'$ and $K-K'$ represent the stress-concentration factors for biaxial tension and pure shear,

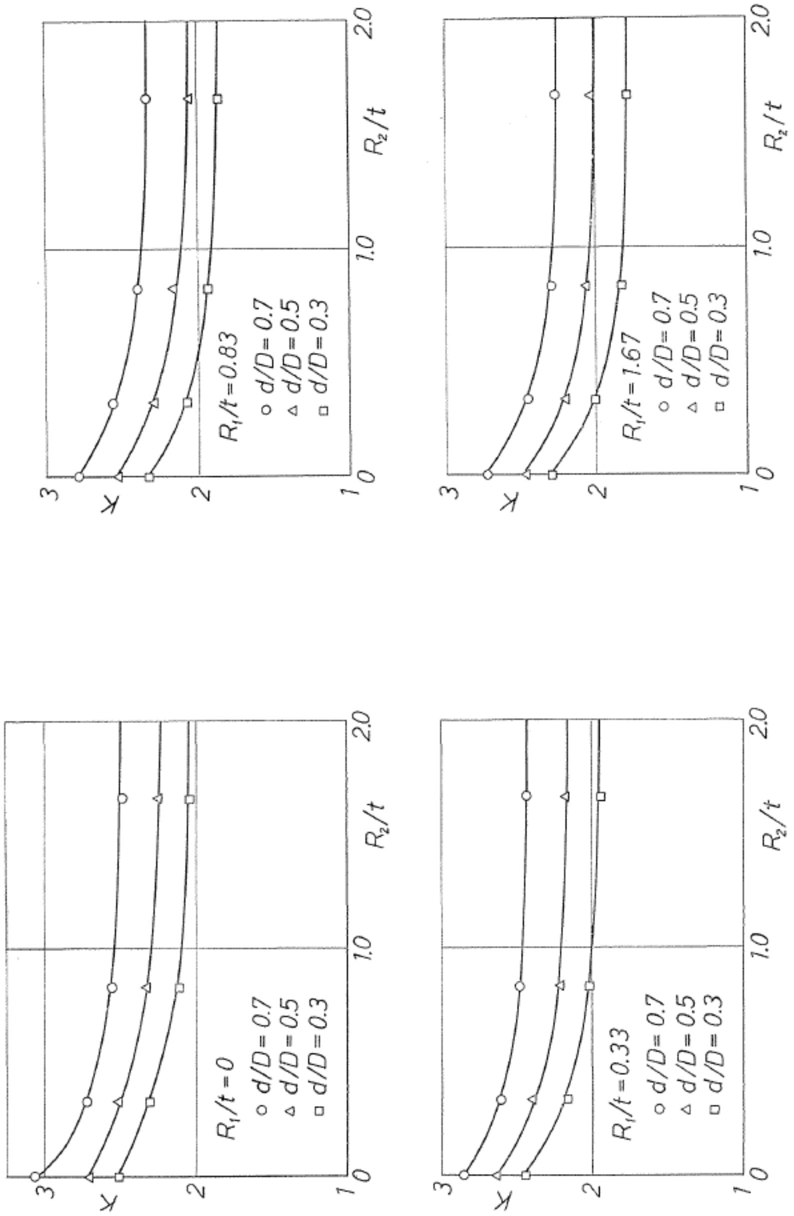

FIG. 6. Stress-concentration factor K for $h/t=3$.

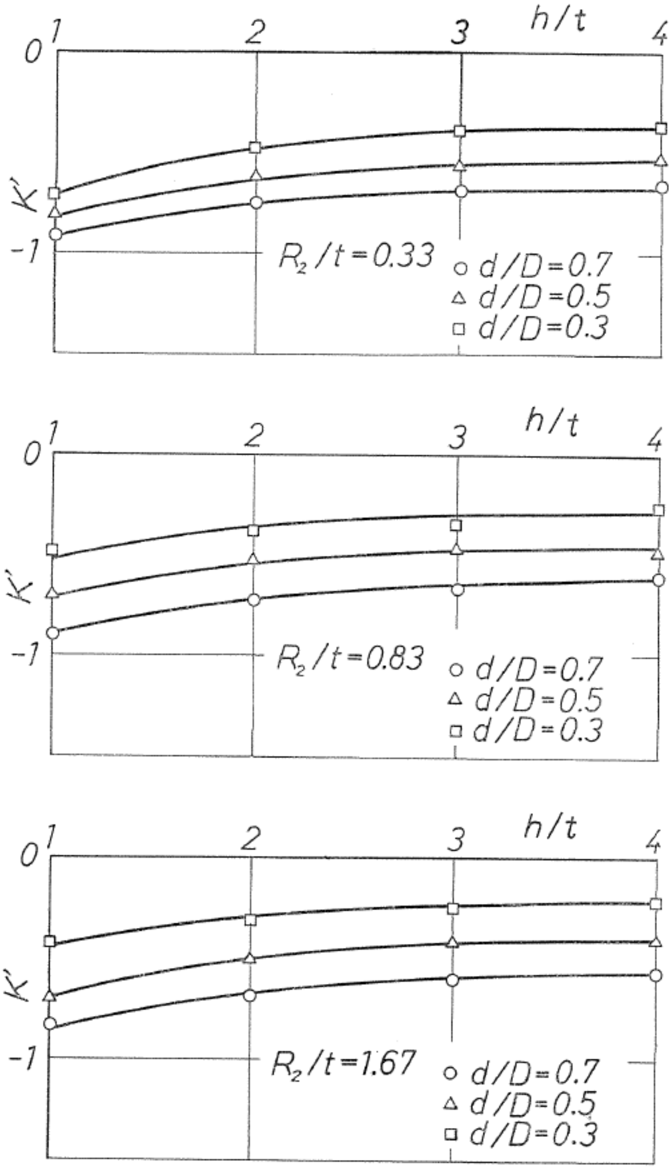

FIG. 7. Stress-concentration factor K' for $R_1/t=0.83$.

respectively. In the figure, the factor $K+1/2K'$ may be available for design data of reinforcement in cylindrical pressure vessels with small openings.

Acknowledgment

The authors wish to express their thanks to Mr. Yoshio Kurisu for his able assistance in performing the experiment.

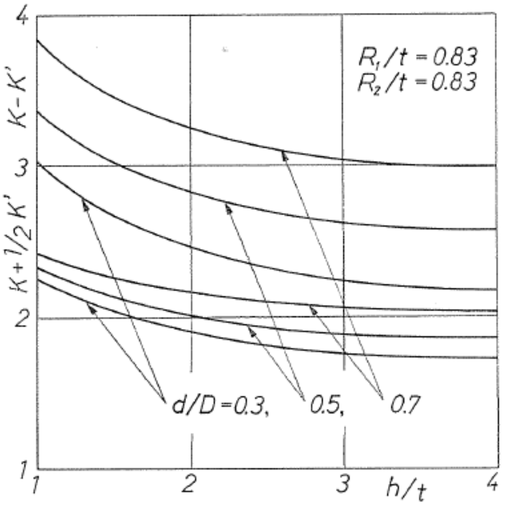

FIG. 8. Stress-concentration factors $K+1/2\,K'$ and $K-K'$

References

1) J. B. Mantle, Photoelastic Analysis of Reinforced Stress Raisers, Proc. Soc. Exper. Stress Analys., **Vol. 1**, No. 2, 1954, p. 161.
2) K. Lingaiah, W. P. T. North, and J. B. Mantle, Photoelastic Analysis of an Asymmetrically Reinforced Circular Cut-out in a Flat Plate Subjected to Uniform Unidirectional Stress, Exper. Mech., **Vol. 6**, No. 12, 1966, p. 617.
3) M. Seika, K. Isogimi, and Y. Kurisu, Photoelastic Investigation of the Maximum Stress in an Infinite Plate with an Asymmetrically Reinforced Circular Hole under Uniaxial Tension, Trans. Japan Soc. Mech. Eng., **Vol. 34**, No. 267, 1968, p. 1885.
4) K. Isogimi and K. Miyake, Photoelastic Investigation of the Maximum Stress in an Infinite Plate with an Asymmetrically Reinforced Circular Hole under Uniaxial Tension (2nd Report, Effects of a Boss with Fillet). Trans. Japan Soc. Mech. Eng., **Vol. 35**, No. 278, 1969, p. 1981.
5) S. Timoshenko and J. N. Goodier, Theory of Elasticity, McGraw-Hill Book Company, Inc., New York, 1951, p. 81.